Precision experiments on gravity by atom interferometry

PRECISION EXPERIMENTS ON GRAVITY BY ATOM INTERFEROMETRY

F. SORRENTINO[1,2], A. ALBERTI[1], L. CACCIAPUOTI[3], M. DE ANGELIS[2], G. FERRARI[1], A. GIORGINI[1,4], V. V. IVANOV[1], N. POLI[1], M. PREVEDELLI[5], G. ROSI[1], M. SCHIOPPO[1], G. M. TINO[1,*]

[1] *Dipartimento di Fisica and LENS-Università di Firenze - INFN, via Sansone 1*
Polo Scientifico, I-50019 Sesto Fiorentino (Firenze) Italy
[2] *Istituto di Cibernetica CNR, Pozzuoli (NA) Italy*
[3] *ESA Reasearch and Scientific Support Department, ESTEC, Noordwijk, The Netherlands*
[4] *Also at: Dipartimento di Fisica, Università di Napoli, Italy*
[5] *Permanent address: Dipartimento di Chimica Fisica e Inorganica, Università di Bologna, Italy*
[*] *E-mail: guglielmo.tino@fi.infn.it*

We present two experiments based on matter-wave interferometry with ultracold atoms to determine the gravitational constant G and to test the Newtonian gravitational law at micrometric distances. We also present ongoing experiments towards the realization of transportable atom interferometers for applications in geophysics and in space.

1. Introduction

The field of laser cooling and manipulation of atoms has been one of the most active in physics in recent years. Atoms from a room-temperature vapour can be cooled to temperatures as low as a few nanokelvin. At such low temperatures the wave properties of the atoms become relevant, giving rise to completely new phenomena such as Bose-Einstein condensation, and allowing to perform experiments where the matter waves interfere just as usual waves do. In the last decade of 20th century, new techniques based on atom interferometry have been developed for the measurement of inertial forces, finding important applications both in fundamental physics and in applied research. The remarkable stability and accuracy that atom interferometers have reached for acceleration measurements can play a crucial role for geophysics. Atom interferometry is used for precise measurements of gravity acceleration [1], Earth's gravity gradient [2,3] and rotations [4]. Applications to metrology and fundamental physics include the determination of the gravitational constant G, measurement of the fine-structure constant, tests of general relativity and Newton's gravitational law. Possible schemes to detect gravitational waves with atom interferometers are under study.

Despite their very recent advent, atom interferometry inertial sensors have already demonstrated excellent sensitivity and accuracy. In the future, application in microgravity environment will allow taking full advantage of the potential sensitivity of atom interferometers [5].

In this paper we present the general principles of operation of atom interferometers and outlines. We also outline future perspectives for accurate gravity measurement for environmental monitoring and space applications.

2. Matter-wave interferometry inertial sensors with cold atoms: basic principles

Matter-wave interference with neutral atoms was first demonstrated in 1991 [6-9]. In analogy to optical interferometers, atomic wave packets are split and recombined giving rise to an interference signal. An overview of basic principles and seminal theoretical and experimental work can be found in [10].

Important applications of atom interferometers, which are most relevant to this paper, lay in the field of inertial sensing. In principle, atom interferometers can be much more sensitive to inertial forces than the corresponding sensors based on optical interferometry. For a given change of gravity acceleration, the phase shift $\Delta\phi_{mw}$ of a matter-wave interferometry gravimeter is larger than the phase shift $\Delta\phi_{ph}$ of an optical interferometry gravimeter with equal size by a factor

$$\frac{\Delta\phi_{mw}}{\Delta\phi_{ph}} = \left(\frac{c}{v}\right)^2 \tag{1}$$

where c is the speed of light and v is the particle velocity in the matter-wave interferometer. Thus the theoretical gain in sensitivity of a matter-wave gravimeter can be as high as $10^{11} \div 10^{17}$, depending on the particle velocity. Similarly, for Sagnac gyroscopes with equal enclosed area, the ratio of phase shift per given rotation rate is:

$$\frac{\Delta\phi_{mw}}{\Delta\phi_{ph}} = \frac{c}{v}\frac{\lambda_{ph}}{\lambda_{mw}} \tag{2}$$

where $\lambda_{mw} = h/mv$ is the De Broglie wavelength of the particles in the matter-wave interferometer, and λ_{ph} is the wavelength in the optical interferometer. Again, the theoretical gain in sensitivity can be as large as $10^{10} \div 10^{11}$ using atomic matter-waves instead of visible light. However, the intrinsic sensitivity advantage of atom interferometers is reduced in view of technical considerations. Better beam-splitters are available for light than for atoms, and the effective size of the interferometer can be increased by high finesse mirrors in optical cavities or multiple fibre turns in fibre-optic gyros. In the future, progress in atom optics will probably result in much larger effective size for atom interferometers. In fact, laboratory matter-wave inertial sensors are already competitive with the best optical or mechanical counterparts [1,4,11]. In the following, we will mainly focus on applications of atom interferometers to acceleration sensing, For the equally interesting field of atomic rotation sensors, the reader may refer for instance to [4,11].

Different schemes can be used for splitting, reflecting and recombining the atoms and the atom optics components can be either material structures [6,7] or light fields [8,9,]. In this section we discuss two different schemes, based on the interaction between ultracold atoms and laser fields, which are relevant for the experiments described in this paper.

Light-pulse atom interferometers [1÷3], are based on transitions between two long-lived atomic states, such as the ground-state hyperfine levels of alkali atoms. By inducing Raman transitions between internal states with a laser field [12], the momentum recoil produces a spatial separation, and the internal and external states of the atoms become entangled. Two counter-propagating beams, with propagation vectors k_1 and k_1, whose frequency difference is resonant with the atomic two-level system, can drive a two-photon Raman transition. The internal state of the atom and its momentum are always coupled, as a consequence of momentum and energy conservation in the system atom + photons.

Alkali atoms collected from the background vapour using laser cooling and trapping methods are pumped in one of the hyperfine states of the atomic ground state. The atoms are left in free fall, either by simply releasing them from the trap or by launching them in fountain configuration as illustrated in fig. 1; then optical pulses are used to stimulate Raman transitions between two different hyperfine states during the flight. These light pulses act on the atom matter-waves in the same way as mirrors and beam splitters act on the light-wave in an optical interferometer. If the initial population is in one single internal state, a $\pi/2$ Raman pulse produces a 50% splitting into the two states with a momentum difference, giving a spatial separation and thus acting as a 50% beam-splitter; a π Raman pulse reverses the atomic population and produces a momentum change, thus acting as a mirror.

A simple Mach-Zender interferometer is obtained with a $\pi/2$-π-$\pi/2$ sequence of three equidistant pulses, as illustrated in fig. 1. It can be shown that if such a pulse sequence is applied with wave-vector parallel to the mean atomic velocity, the resulting phase difference accumulated along the atom interferometer paths is given by

$$\Delta\phi = k_{eff} a T^2 \tag{3}$$

where a is the acceleration of the atoms along the wave-vector of lasers, $k_{eff} = k_2 - k_1 \cong -2k_1$ and T is the temporal separation between two interferometer pulses. The sensitivity of the method therefore increases with the interrogation time and this is the reason to use cold atoms. An important advantage of this atom interferometer scheme is that it is intrinsically free of instrumental drifts thus allowing integration over very long time intervals to increase sensitivity. Eqn. (3) also shows that a significant increase of the sensitivity can be achieved if each pulse of the sequence is replaced by a sequence of pulses [13], thus increasing the spatial separation between the two parts of the atomic wave-packet.

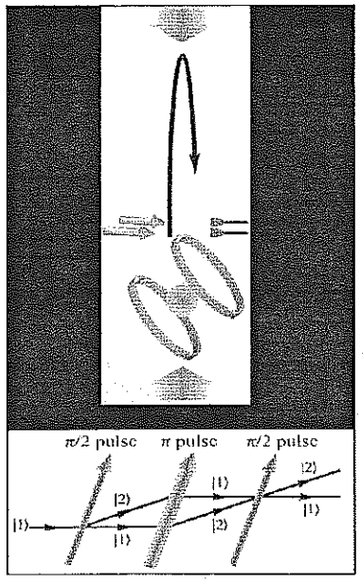

Figure 1. Above is shown a scheme of an atom interferometry gravimeter in fountain configuration; atoms are first collected in a megneto-optical trap, then are launched upwards and interrogated by a sequence of Raman pulses; finally, the population of internal states is measured by fluorescence detection. Below is illustrated the principle of the Raman light-pulse interferometer.

The output phase $\Delta\phi$ of the atom interferometer in eqn. (3) can be read out by measuring the population of the two hyperfine levels through fluorescent detection: the population ratio has a sinusoidal dependence on $\Delta\phi$.

The Raman transition between two internal states are induced by two laser beams whose frequency difference is phase-locked to a stable microwave source. This must ensure a precise control of the relative phase, since the atom interferometer maps relative phase fluctuations between the two optical fields into acceleration fluctuations. Another crucial element of the interferometer is the mirror used to retro-reflect the Raman laser beams. This mirror plays the role of an inertial reference during the measurement. The two laser beams can be arranged to travel along the same path and only vibrations of this mirror can affect the relative phase. Therefore this mirror needs to be stabilized using active low-frequency vibration isolation systems to reduce vibrations in the 0.1-10 Hz range. The better the mirror vibration isolation, the larger can be the time T between pulses and the resulting sensitivity.

One important advantage of the atom interferometer here described results in implementing a gravity gradiometer. In fact, by using the same optical and laser set-up to interrogate two vertically displaced atomic clouds in free fall, several possible source of perturbation (such as laser relative phase noise, vibration of the retro-reflecting mirror, etc.) are reduced to common mode, allowing an excellent degree of noise rejection. The calibration for the two accelerometers is referenced to the wavelength of a single pair of frequency-stabilized laser beams, and is identical for both accelerometers. This provides long-term accuracy.

Although the Raman light-pulse atom interferometry scheme just described has given so far the best results in terms of acceleration sensitivity, interesting applications have also been demonstrated with a different approach based on the off-resonant interaction with optical lattices. When a sample of atoms interacts with a laser standing wave generated by two counter-propagating laser beams, the optical lattice acts as a diffraction gratings for the atoms. In such regular structures created by interfering laser beams the atoms can be trapped by dipole force. An interesting description of such system can make use of the formalism of solid-state physics. In particular, under the influence of a periodic potential and a weak uniform force, the atomic quasi-momentum changes periodically across the first Brillouin zone, a phenomenon known as Bloch oscillations [14]. The period of such oscillations is determined by the time spent to scan the full width Δk of the Brillouin zone, as illustrated in fig. 2. The time derivative of quasi-momentum is given by the weak uniform force F times $\hbar^{-1}$, thus the frequency of Bloch oscillations can be simply expressed as

$$\nu_B = \frac{F}{\hbar \Delta k} = \frac{F \lambda_L}{2h} \tag{4}$$

where λ_L is the wavelength of the light producing the lattice, and h is the Planck constant. Since λ_L can be known with high precision, the resulting force along the lattice axis can be determined by measuring the Bloch frequency ν_B. With a vertically oriented optical lattice one can measure the gravitational acceleration through $F = mg$ [15]. The precision of acceleration measurements depends on the resolution to which the Bloch frequency can be determined. Sensitivity to g in the ppm range has been demonstrated in [15]; coherent delocalization of the atomic wave-packet along the lattice axis has been used in [16] to improve sensitivity, which however is still quite low as compared to Raman light-pulse interferometry. On the other hand, the possibility to observe Bloch oscillations is not limited to two-level atoms. More importantly, such technique applies to trapped atoms in a very small volume of micrometer scale, giving a local acceleration measurement.

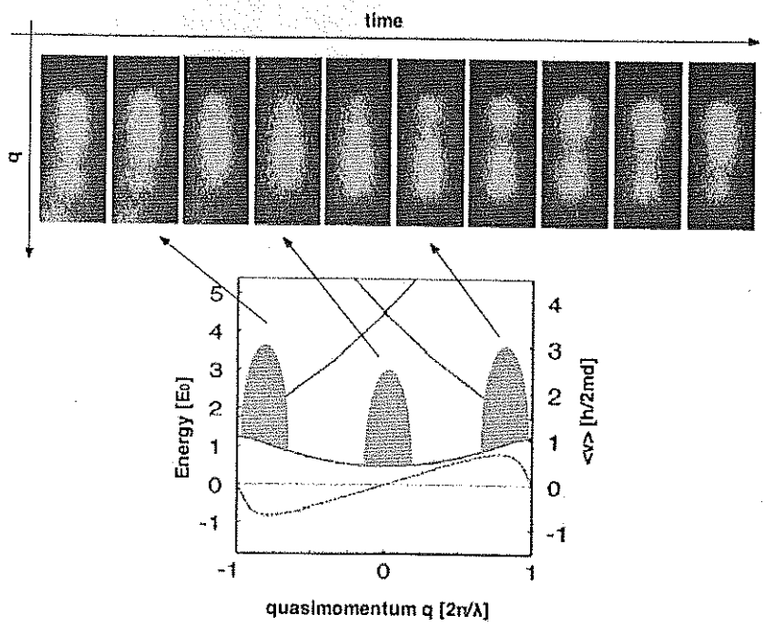

Figure 2. Bloch oscillations of atoms in an optical lattice under the influence of a small uniform force. Upper part shows the momentum distribution of atomic sample at different times; the atomic quasi-momentum has a linear drift with time, before reaching the edge of the Brillouin zone; then it is reflected to the other edge.

3. Measurement of G by Raman light-pulse atom interferometry

One of the oldest and most intriguing problems in metrology is the determination of the gravitational constant. The extreme weakness of the gravitational interaction and the impossibility of shielding the effects of gravity make it difficult to measure G while keeping systematic effects well under control. The CODATA-2006 recommended value for G is $6.67428(67)\cdot10^{-11}$ $m^3kg^{-1}s^{-2}$ [17]. G is still affected by an uncertainty of 100 ppm, much higher than that of any other fundamental constant, and the results of most recent experiments differ by several hundreds ppm. Among the possible sources for this unexplained discrepancy one in particular appears mostly critical. The majority of the experiments performed so far are based on macroscopic suspended masses. Systematic effects and parasitic couplings in suspending fibres could be responsible for the observed discrepancies.

Our approach is to use atom interferometry to perform precision measurements of the gravitational interaction between point-like test masses, i.e. atoms, and well characterized source masses [3,18]. In the MAGIA experiment (Misura Accurata di G mediante Interferometria Atomica) we apply a Raman interferometer to measure the differential acceleration experienced by two samples of laser-cooled rubidium atoms under the influence of nearby tungsten masses [19]. From the knowledge of the source mass distribution it is then possible to determine the value of G. The experiment was accurately designed in order to have a better control on the systematic errors and to achieve an uncertainty of 10^{-4}.

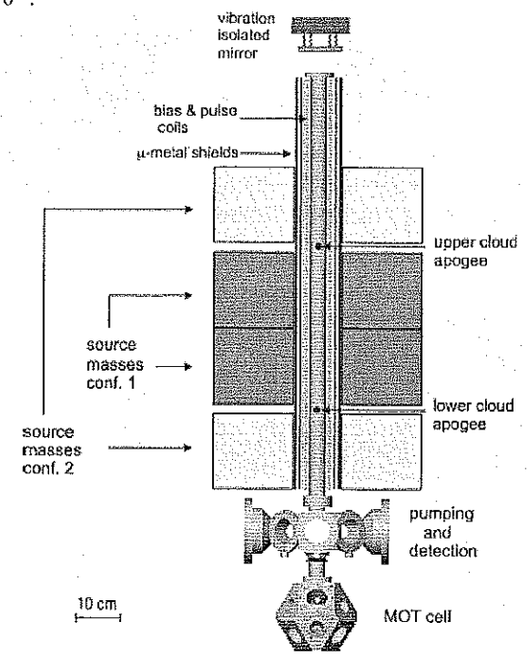

Figure 3. Schematic drawing of the MAGIA apparatus.

Two sets of source masses are symmetrically arranged in a cylindrical geometry around the vacuum tube where atoms are launched in a fountain configuration, as shown in fig. 3. For the determination of G, the source masses signal is detected as variation on the gradient of gravity acceleration. We apply a $\pi/2$-π-$\pi/2$ sequence of Raman pulses, as illustrated in section 2. If g_{DW} (g_{UP}) is the gravity acceleration value at the height of the lower (upper) interferometer, the relative phase shift is $\Delta\phi = k_{eff}(g_{DW} - g_{UP})T^2$. This method has the major advantage of being highly insensitive to noise sources appearing in common mode on both interferometers. In particular, any spurious acceleration induced by vibrations or seismic noise on the common reference frame identified by the vertical Raman beams is efficiently rejected by the differential measurement technique.

We implement a double differential scheme to determine G. The measurements of gravity gradient are repeated twice with atom clouds in the same point but the two source masses in different positions, so that all contributions that are constant in time during the measurement cycle, like rotational or gradient contribution, should cancel out. Fig. 4 shows typical measured data, where the effect of source mass displacement is clearly detected as differential phase shift between the upper and lower interferometers.

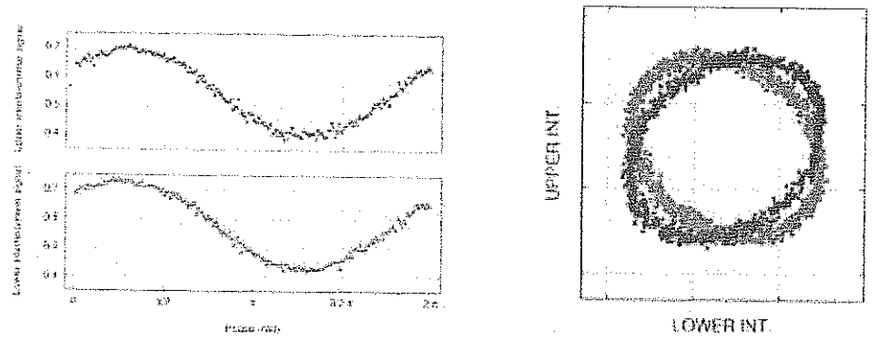

Figure 4. Gravity gradiometer measurement; plots on the left are the fringes obtained as output from the upper and lower interferometers when the Raman laser phase is scanned; plots on the right are ellipses obtained by plotting the phase of the upper interferometer versus the phase of the lower one; the two ellipses shown refer to the two different positions of the source masses. From the eccentricity and the rotation angle of the ellipses the gravity gradient is computed.

In our experiment specific efforts have been devoted to the control of systematic effects related to atomic trajectories, positioning of source masses, and stray fields. In particular, the high density of tungsten and the distribution of the source masses are crucial in our experiment to compensate for the Earth gravity gradient and reduce the sensitivity of the measurement to the initial position and velocity of the atoms. The measurement, repeated for two different configurations of the source masse, is modelled by a numerical simulation, which takes into account the mass distribution and the evolution of atomic trajectories. The comparison of measured and simulated data provides the value of the Newtonian gravitational constant G. After an analysis of the error sources affecting our measurement, we obtain a value of $G=6.667\cdot10^{-11}$ $m^3kg^{-1}s^{-2}$, with a statistical uncertainty of $\pm0.011\cdot10^{-11}$ $m^3kg^{-1}s^{-2}$ and a systematic uncertainty of $\pm0.003\cdot10^{-11}$ $m^3kg^{-1}s^{-2}$. Our measurement is consistent with the 2006 CODATA value within one standard deviation. The main contribution to the systematic error on the G measurement derives from the positioning accuracy of the source masses. This error will be reduced by about one order of magnitude by measuring the position of the tungsten cylinders with a laser tracker.

4. Force measurements at small length scale using Sr atoms in optical lattices

The use of ultracold atoms for studying forces at small length scales has been recently addressed by several groups, both experimentally [15] and theoretically [20]. Besides the technological implications [21], measuring forces at short distance has become attractive for several research fields in physics, spanning from Casimir effect [22] to tests of Newtonian gravity at micrometer distance [23,24].

Recent theories beyond the Standard Model predict deviations from the Newton gravitational law; such deviations are usually described by adding a Yukawa-type term to the interaction between two point masses, so that the potential is written as

$$-G\frac{m_1 m_2}{r}\left(1+\alpha\cdot e^{-\frac{r}{\lambda}}\right) \qquad (5)$$

where G is the Newtonian gravitational constant, m_1 and m_2 are the masses, and r is the distance between them. The parameter α gives the relative strength of deviations from Newtonian gravity and

λ is its spatial range. Experiments searching for possible deviations have set bounds for the parameters α and λ. Exotic theories predict deviations in the range $\lambda < 1$ mm. Recent results using micro-cantilever detectors lead to extrapolated limits $\alpha < 10^4$ for $\lambda \sim 10$ μm [25], while for distances below 10 μm it was not possible to perform direct experiments so far.

Force sensing at sub-millimeter scale has been achieved with several techniques based on the interaction between mesoscopic objects [23,24,26÷28]. Ultracold atoms offer additional degrees of freedom, and provide a new class of sensors combining good accuracy with high spatial resolution. Although most of the proposed schemes make use of quantum degenerate gases to reach long coherence times for the degrees of freedom under analysis, we demonstrated that excellent performances can be obtained with a classical ultracold gas, by choosing atoms with suited properties [15, 16]. In this respect, ^{88}Sr represents an ideal candidate for precise quantum sensors, as it combines low sensitivity to magnetic fields with remarkably small atom-atom interactions [29].

In this section we describe the all-optical production of a quantum sensor for accurate force measurements with high spatial resolution, based on a sample of ultracold strontium atoms. A promising technique consists in observing the Bloch oscillations of the atomic momentum in a 1-D optical lattice, as described in section 2. By means of laser manipulation techniques, we can place an ultracold ^{88}Sr sample close to a test surface. The coherence of Bloch oscillations is preserved in the vicinity of the surface, and the atom-surface interaction can be detected through a shift in the oscillation frequency. As shown below, higher sensitivity can be obtained by means of coherent delocalization of the atomic wave-function along the optical lattice [16]. The small size and high sensitivity of the atomic probe will allow a model-independent measurement of gravitational interaction at distances of a few μm from the source mass, giving direct access to unexplored regions in the $\alpha - \lambda$ plane.

A scheme of our system is shown in fig. 5. We start the sensor preparation from a sub-μK atomic sample in a magneto-optical trap (MOT). The process of cooling and trapping strontium atoms below the photon recoil limit consists of a double-stage magneto-optical trapping scheme: a "blue MOT" operated on the $^1S_0$-$^1P_1$ transition at 461 nm, with an atomic temperature of few mK, followed by a "red MOT" operated on the $^1S_0$-$^3P_1$ intercombination transition at 689 nm, where the minimum attainable temperature is approximately half the photon recoil limit, i.e. 230 nK. In the final red MOT the shape of the atomic cloud is rather flat, as the atoms sag on the bottom of the ellipsoidal shell where they are in resonance with the Zeeman-shifted laser field in the MOT magnetic quadrupole [30]. The vertical size of the atomic cloud is basically limited by the line-width of the cooling transition.

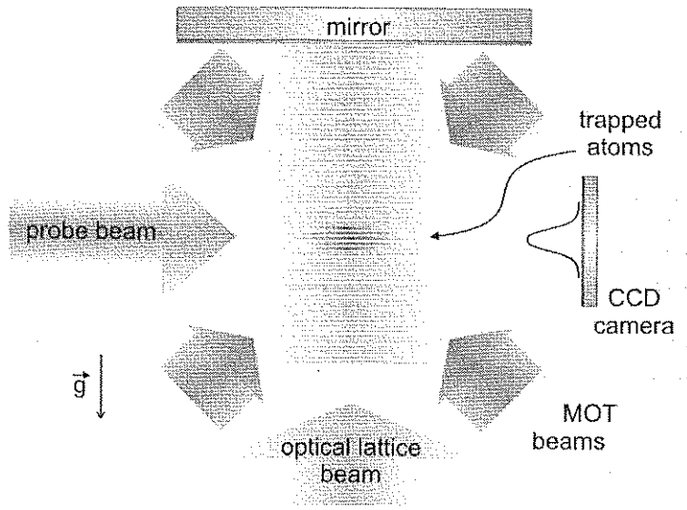

Figure 5. Scheme of the experiment with ^{88}Sr in optical lattice: strontium atoms are first cooled and trapped in a MOT, then are loaded in a vertical optical lattice; the atomic density distribution is measured through absorption imaging; momentum distribution is deduced by time-of-flight measurement.

After trapping into the red MOT we transfer the atoms to a vertical 1-D optical lattice. The standing wave is produced with two counter-propagating laser beams. As reported in ref. [15], when directly transferring the atoms from the red MOT to a vertical optical lattice we obtain a disk-shaped sample with a rms vertical half-width of ~12 μm and a horizontal radius of ~150 μm. We observe Bloch oscillations of the vertical atomic momentum by releasing the optical lattice at a variable delay, and by imaging the atomic distribution after a fixed time of free fall. The coherence time for the Bloch oscillation is 12 s, corresponding to ~ 7000 oscillations. These values are among the highest ever observed for Bloch oscillations in atomic systems.

From the measured Bloch frequency the gravity acceleration along the optical lattice is estimated with a sensitivity of $4 \cdot 10^{-6}$ g at 1 s. The resolution can be largely improved through the use of coherent delocalization of the atomic wave-function, by resonantly driving the optical lattice. We have developed different manipulation methods.

Modulating the axial position of the vertical optical lattice at exact harmonics of the Bloch frequency results in a coherent spreading of the atomic sample along the lattice axis. Coherence of such process is demonstrated by the absence of line broadening effects, i.e. the modulation spectrum is Fourier-limited. Since the quality factor increases with the harmonic order, this effect allows to measure the linear acceleration along the lattice axis with higher resolution, as described in [16]. The method is illustrated in fig. 6, together with experimental results.

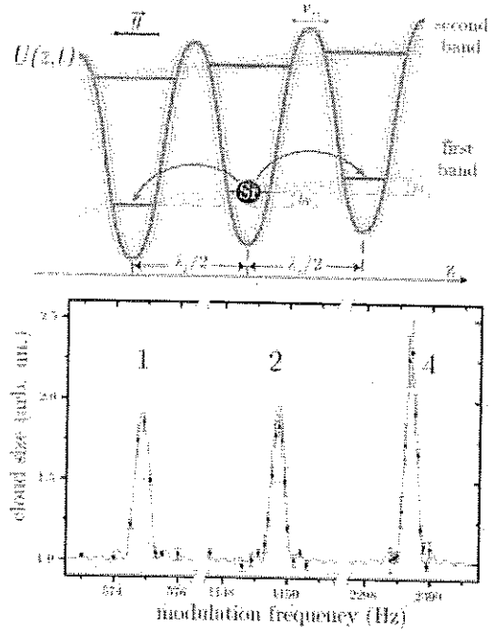

Figure 6. The drawing is an illustration of coherent delocalization method: the axial position of the optical lattice is modulated at a rate close to an harmonic of the Bloch frequency, giving rise to resonant coupling between neighbour lattice sites; the plot shows the axial size of the atomic distribution measured versus the modulation rate: the size is enhanced on resonance due to coherent delocalization.

Modulating the axial position of the vertical optical lattice at a frequency different from that of Bloch oscillations causes a reversible delocalization of the atomic wave-function along the lattice axis. Periodic revival of the initial distribution, with a period given by the detuning of driving frequency from Bloch frequency, is a clear demonstration of the coherence of such process. We have shown that coherence is preserved in time up to tens of seconds, and in space up to the mm range. Spatial delocalization corresponds to shrinking the momentum distribution of the atomic wave-function along the lattice axis, as shown in [31]. Again, a narrower momentum distribution yields a better resolution in measuring the frequency of Bloch oscillations.

The size of the atomic sample gives access to force/acceleration measurements with high spatial resolution, since the atoms are confined in a small region by the optical lattice trap. We developed manipulation techniques to control the position of the atomic sample with nm resolution along the sensitive axis, and to reduce the size of the sample in view of measurements at short distance from surfaces. An optical tweezer was applied to compress the sample to a few microns along the sensitive axis, and an optical elevator was realized to translate the atoms close to a test surface, in order to detect forces arising from atom-surface interactions. Fig. 7 shows precise positioning of atoms close to a test surface by means of the optical elevator, as well as the Bloch oscillations recorded at atom-surface distance of 15 μm; in the same figure we show an in situ image of the atoms compressed with the optical tweezer.

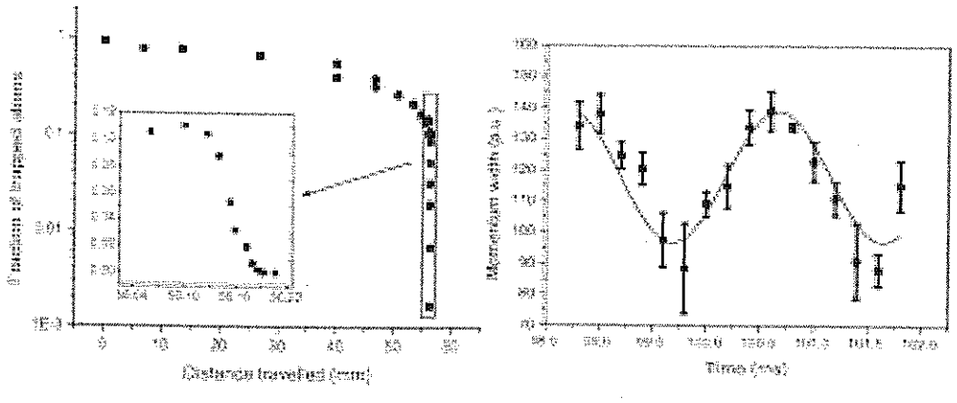

Figure 7. Small length scale measurements; plot on the left shows the fraction of atoms recorded after the elevator round-trip, versus vertical displacement; the inset shows the region close to the test surface; central plot shows the Bloch oscillations of the atomic momentum measured with atoms at a distance of 15 μm from the test surface; on the right is displayed an in-situ absorption image of the atoms trapped in the optical tweezer; untrapped falling atoms are also visible.

These preliminary results suggest that our system may allow to directly test non-Newtonian gravity in the region around $\lambda \sim 5$ μm with a sensitivity to the α value of 10^3, which is more than one order of magnitude lower than the present bounds.

5. Towards a transportable atom interferometer: results and applications

In spite of the relatively recent emergence of matter-wave optics, atom interferometry inertial sensors have already progressed, in a research environment, to the point where their performance is comparable or even better than the best optical or mechanical counterparts. Quantum inertial sensors have the potential for replacing present state-of-the-art technologies in several fields, e.g. for geophysics and space applications. Present research in the field of atom interferometry is following two main lines. New configurations, based for instance on quantum degenerate gases and/or coherent

detection methods, are under study to improve sensitivity; on the other hand, some research groups are working to develop compact and transportable atom interferometers with performance similar to the existing laboratory systems. Prototypes of compact gravimeters/gravity gradiometers have been realized in Stanford and Paris. Our group is involved in these activities in the frame of several European (EU and ESA) and national (INGV) programs. In a joint effort among European research groups, a new portable gravimeter is under construction within a European STREP/NEST project (FINAQS: Future Inertial Atomic Quantum Sensors); the instrument aims to an accuracy in the range of 1 parts in 10^{10}, an order of magnitude improvement over the best current instruments. Interest on application of atomic quantum sensors in space is demonstrated by the activities stimulated by ESA and by national space agencies, CNES, ASI, DLR. In particular, since 2007 ESA is funding a pre-phase A project (SAI Space Atom Interferometer) to exploit the potential of matter-wave sensors in microgravity for the measurement of acceleration, rotation, and faint forces. SAI aims to push the present performances to the limits and to demonstrate this technology with a transportable sensor which will serve as a prototype for the space qualification of the final instrument.

Accurate gravity measurements find applications in many fields of physics: in metrology for both the definition of SI units and a better knowledge of fundamental constants; in high-precision tests of general relativity, in satellite gravity missions for the geoid mapping, and in geophysical studies [32]. Users' interest in terrestrial gravity measurements are in high resolution prospecting for resource exploration, monitoring of man-induced processes, high resolution geoid mapping (or positioning), investigation of subsurface 6 mass redistribution at local (e.g. volcanoes and geothermal systems), regional (post-glacial rebound) and global scales (Earth's mantle and core). Data from gravity surveys at the Earth's surface are usually processed relatively to a network of reference stations. The systems of stations shows an accuracy decay during time, which is mostly due to decay of the relative instruments (like spring gravimeter) used. For such stations, therefore, more is the need for instruments monitoring high accuracy over time. Recently, continuous micro-gravimetric observations have found a further, important field of application to volcano monitoring. It appears that mass redistribution in volcanic systems occur over time scales spanning the $10^2 \div 10^6$ s interval (i.e. minutes to months), and have amplitudes ranging from 10 μgal up to hundreds of μgal (1 μgal= 10^{-9} *g*), which means that a long term stability instrument is needed to have a resolution of 1÷10 μgal over 1 year. Subsurface mass redistributions of geodynamical interest occurs over time scales, spanning the $10^6 \div 10^8$ s interval (i.e. days to years), and produce gravity variations whose amplitude ranges from a few μgal up to hundreds of μgal. Although subtle, these variations generally precede other surface-detectable signals such as strain deformations and/or seismic ground shaking. Taken all together, these considerations thus indicate that the continuous observation of the local gravity field using sensitive instrumentation with μgal accuracy and over long periods (years) is a major goal to be attained toward a better understanding of geodynamic processes and a successful assessment of earth- quake and volcanic hazards.

The enormous sensitivity of atomic sensors for accelerations and rotations scales with the measurement time, during which the matter wave accumulates the phase along the interferometer trajectories, as can be seen for instance eqn. (3). Motivation for laser cooling is therefore to reach lower temperatures for a maximum extension of the measurement time. In such case, since the experiments are better performed with atoms in free fall to avoid perturbations due to any confining force, the observation time will be ultimately limited by the gravitational acceleration. For this reason, future experiments in microgravity are expected to further improve the performance of atomic quantum sensors. A space gravity gradiometer in microgravity conditions where interrogation time up to 10 s could in principle achieve sensitivity better than 10^{-12} s^{-2} at 0.1 Hz.

Possible applications of atom interferometry in space are interdisciplinary, spanning from fundamental physics (tests of general relativity, search for new forces, tests of atom neutrality, etc.), to metrology (definition of kg, measurement of *G* and h/m), astronomy and space navigation (inertial references), prospecting for resources and major Earth-science themes (i.e. satellite missions to map the geoid), GALILEO and LISA technology.

References

1. Peters, A., Chung, K. Y., and Chu, S., 1999, Nature 400 849.
2. McGuirk, J. M., Foster, G. T., Fixler, J. B., Snadden, M. J., and Kasevich, M. A., 2002, Phys. Rev. A, 65, 033608.
3. Lamporesi, G., Bertoldi, A., Cacciapuoti, L., Prevedelli, M., and Tino, G. M., 2008, Phys. Rev. Lett., 100, 050801.
4. Gustavson, T. L. , Landragin, A., and Kasevich, M. A., 2000, Class. Quantum. Grav., 17, 2385.
5. Tino, G. M., 2007, Nucl. Phys. B, 113, 289.
6. Carnal, O., and Mlynek, J., 1991, Phys. Rev. Lett., 66 2689.
7. Keith, D. W., Ekstrom, C. R., Turchette, Q. A., and Pritchard, D. E., 1991, Phys. Rev. Lett., 66, 2693.
8. Riehle, F., Kisters, Th., Witte, A., Helmke, J., and Bordè, Ch. J., 1991, Phys. Rev. Lett., 67, 177.
9. Kasevich, M., and Chu, S., 1992, Appl. Phys. B, 54 321.
10. Cronin, A. D., Schmiedmayer, J., and Pritchard, D. E., 2007, arXiv:0712.3703.
11. Durfee, D. S., Shaham, Y. K., and Kasevich, M. A., 2007, Phys. Rev. Lett., 97, 240801.
12. Moler, K., Weiss, D. S., Kasevich, M., and Chu, S., 1992, Phys. Rev. A, 45, 342.
13. McGuirk, J. M., Snadden, M. J., and Kasevich, M. A., 2000, Phys. Rev. Lett., 85, 4498.
14. Bloch, F., 1929, Z. Phys., 52, 555.
15. Ferrari, G., Poli, N., Sorrentino, F., and Tino, G. M., 2006, Phys. Rev. Lett., 97, 060402.
16. Ivanov, V. V., Alberti, A., Schioppo, M., Ferrari, G., Artoni, M., Chiofalo, M., and Tino, G. M., 2008, Phys. Rev. Lett., 100, 043602.
17. Mohr, P. J., Taylor, B. N., and Newell, D. B., 2008, CODATA Recommended Values of the Fundamental Physical Constants: 2006.
18. Bertoldi, A., Lamporesi, G., Cacciapuoti, L., de Angelis, M., Fattori, M., Petelski, T., Peters, A., Prevedelli, M., Stuhler, J., and Tino, G. M., 2006, Eur. Phys. J. D, 40, 271.
19. Lamporesi, G., Bertoldi, A., Cecchetti, A., Duhlach, B., Fattori, M., Malengo, A., Pettorruso, S., Prevedelli, M., and Tino, G. M., 2007, Rev. Sci. Instrum., 78, 075109.
20. Dimopoulos, S., Geraci, A. A., 2003, Phys. Rev. D, 68, 124021.
21. Chan, H. B., Aksyuk , V. A., Kleiman, R. N., Bishop, D. J., and Capasso, F., 2001, Phys. Rev. Lett., 87, 211801.
22. Harber, D. M., Obrecht, J. M., McGuirk, J. M., and Cornell, E. A., 2005, Phys. Rev. A, 72, 033610.
23. Long, J. C., Chan, H. W., Churnside, A. B., Gulbis, E. A., Varney, M. C. M., and Price, J. C., 2003, Nature, 421, 922.
24. Smullin, S. J., Geraci, A. A., Weld, D. M., Chiaverini, J., Holmes, S., and Kapitulnik, A., 2005, Phys. Rev. D, 72, 122001.
25. Weld, D. M., Xia, J., Cabrera, B., and Kapitulnik, A., 2007, arXiv:0801.1000.
26. Bressi, G., Carugno, G., Onofrio, R., and Ruoso, G., 2002, Phys. Rev. Lett., 88, 041804.
27. Hoyle, C. D., Kapner, D. J., Heckel, B. R., Adelberger, E. G., Gundlach, J. H., Schmidt, U., and Swanson, H. E., 2004, Phys. Rev. D, 70, 042004.
28. Decca, R. S., Fischbach, E., Klimchitskaya, G. L., Krause, D. E., Lòpez, D., and Mostepanenko, V. M., 2003, Phys. Rev. D, 68, 116003.
29. Sorrentino, F., Ferrari, G., Poli, N., Drullinger, R. E., and Tino, G. M.,, 2006, Mod. Phys. Lett. B, 20, 1287.
30. Loftus, T. H., Ido, T., Ludlow, A. D., Boyd, M. M., and Ye, J., 2004, Phys. Rev. Lett., 93, 073003.
31. A. Alberti and V. V. Ivanov and G. M. Tino and G. Ferrari, 2008, arXiv:0803.4069.
32. de Angelis, M., Bertoldi, A., Cacciapuoti, Giorgini, A., L., Lamporesi, G., Prevedelli, M., Saccorotti, G., Sorrentino, F., and Tino, G. M., 2008, Meas. Sci. Technol. (to be published).

G-PISA GYROLASER

J. BELFI[1,2], N. BEVERINI[1,2,3], F. BOSI[2], G. CARELLI[1,2,3], A. DI VIRGILIO[2], R. GRAHAM[1,*], E. MACCIONI[1,2,3], A. PORZIO[4], U. SCHREIBER[5], S. SOLIMENO[4], F.SORRENTINO[6], A. VELIKOSELTSEV[5]

[1] *Dipartimento di Fisica Università di Pisa, largo Bruno Pontecorvo 3, I-56127 Pisa, Italy*
[2] *INFN, Sezione di Pisa, Italy*
[3] *CNISM, Unità di Pisa, Italy*
[4] *Dipartimento di Fisica Università "Federico II", and CNISM, Unità di Napoli, Napoli, Italy*
[5] *Forschungseinrichtung Satellitengeodaesie der Technischen Universitaet Muenchen Fundamentalstation Wettzell - Germany*
[6] *Dipartimento di Fisica Università di Firenze, Sesto Fiorentino, Italy*

G-Pisa is an experiment which will investigate the possibility to operate a laser-gyro with area less than 1 m^2 and high sensitivity in order to use a laser-gyro to improve the performances of the mirrors suspension of the gravitational wave antenna Virgo. The experimental set-up consists of a 4 mirrors square cavity, the mechanical drawing allows us to scale the area from 2 down to 0.81 m^2. We collaborate with the groups from New Zealand and Germany which have so far built several large frame lasers-gyro used to monitor the fluctuation of the Earth rotation speed, these devices have areas of the order of 20-800 m^2 and work fixed to the ground. A more compact system has several advantages: it is cheaper, can be easily moved and can be used to monitor the orientation of mobile equipments.

1. Introduction

Laser-gyros are devices sensitive to inertial angular motion. They are based on the Sagnac effect: in a closed cavity rotating at angular velocity Ω the two counter propagating beams complete the path at different times. Different kinds of such devices have been developed mainly for aircraft, ship and submarine navigation. They are only sensitive to angular velocity and entirely insensitive to translational velocity. We distinguish between passive (fiber optic gyros) and active (ring lasers) Sagnac interferometers. Passive devices measure the phase shift between the two beams, while the active ones measure the frequency difference, an inherently more accurate measure. Small fiber gyros typically used for navigation have a resolution of 10^{-8} rad/s, while the large ring laser gyros used in geophysics and geodesy have a sensitivity at the level of 10^{-12} rad/s. In the following we will focus on active ring lasers and will call them simply gyros. One application of large gyros is the monitoring of the variations of Earth rotation speed. Up to now the reached resolution is 10^{-8} of the Earth rotation, integrating the signal for several hours [1-5]. Mode locking between the two counter-propagating modes of the laser is the major problem of small ring lasers; technical tricks, like rate biasing or dithering, have to be applied to overcome this issue. In large gyros the rate bias induced by the Earth rotation is enough to avoid mode locking. The orientation with respect to the Earth axis is important since the induced signal is proportional to the scalar product between the normal of the gyro area and Earth axis, see equation (1). For horizontal gyros the signal is zero at the equator and maximum at the pole; at intermediate latitudes, horizontal and vertical cavities work fine. The Sagnac frequency i.e. the beat signal between the two output beams is:

$$\delta\phi = \frac{4A}{\lambda P}\cdot\vec{n}\cdot\vec{\Omega} + \phi_\rho \qquad (1)$$

where A and P are the area and perimeter of the cavity respectively, λ is the wavelength of the laser beam, $\vec{n}$ the normal vector on the plane of the ring cavity and $\vec{\Omega}$ the induced vector of rotation, with Earth rotation being at least one contributor; ϕ_ρ is denoting additional, usually very small, contributions to the Sagnac frequency due to non-reciprocal effects in the laser cavity, such as Fresnel drag [6].